SACLANTCEN Memorandum SM – 159

SACLANTCEN Memorandum
SM – 159

SACLANT ASW RESEARCH CENTRE MEMORANDUM

AN ANALYSIS OF HIGH-FREQUENCY AMBIENT NOISE

by

Lewis J. LLOYD and Maurice J. DAINTITH

1 OCTOBER 1982

NORTH
ATLANTIC
TREATY
ORGANIZATION

LA SPEZIA, ITALY

Published by

STI

SACLANTCEN MEMORANDUM SM-159

NORTH ATLANTIC TREATY ORGANIZATION

SACLANT ASW Research Centre
Viale San Bartolomeo 400, I-19026 San Bartolomeo (SP), Italy.

tel: national 0187 560940
international + 39 187 560940

telex: 271148 SACENT I

AN ANALYSIS OF HIGH-FREQUENCY AMBIENT NOISE

by

Lewis J. Lloyd and Maurice J. Daintith

1 October 1982

This memorandum has been prepared within the SACLANTCEN Systems Research Division as part of Project O2.

L. F. Whicker

L.F. WHICKER
Division Chief

TABLE OF CONTENTS

List of Figures

AN ANALYSIS OF HIGH-FREQUENCY AMBIENT NOISE

by

Lewis J. Lloyd and Maurice Daintith

ABSTRACT

Because of the high values of absorption and bottom-reflection losses, ambient noise in shallow water at frequencies above 30 kHz is considered to result almost entirely from wind and rain activity at the local sea surface. The ambient noise is thus effectively produced by a series of small radiators distributed over a plane surface, with the level and directionality of the sources being dependent on wind speed, rainfall, and frequency. In order to assess the form of signal processing to use in a high-frequency ambient-noise field, analytical expressions have been developed for the noise power in an omnidirectional hydrophone, for the horizontal and vertical spatial correlation functions, and for the noise power in an unshaded rectangular array.

INTRODUCTION

In the early studies of anisotropic noise fields the effects of absorption loss and bottom acoustic interactions were neglected <1,2>. Omission of the absorption loss implies that the analysis relates to low frequencies, in which case bottom interactions should be included. Recent studies by Kuperman and Ingenito <3> and Buckingham <4> apply to low frequencies, since bottom interactions are incorporated but the absorption loss is omitted.

In the study of high-frequency ambient noise in shallow water at frequencies above 30 kHz the absorption loss should be included, since it can be an appreciable part of the propagation loss; for example, the attenuation parameter α is equal to 13 dB/km at 50 kHz for a temperature of 15.5°C. However, bottom-reflection losses are of the order of 15 dB and more per bounce for grazing angles between 10° to 90°, and propagation in the sea-bed is negligible, so that bottom interactions can be neglected.

In consequence, a good representation of the high-frequency ambient-noise field in shallow water is given by assuming a number of small independent noise radiators spread over the sea surface, with there being no coupling back into the sea via the sea-bed. The level and directionality of the noise radiators is assumed to be a function of the wind and rain activity on the local sea surface and of frequency. Because bottom interactions are neglected the propagation out to ranges of about three times the water depth is reasonably well defined by straight-line ray paths and a propagation loss given by $20 \log r + \alpha r$.

This memorandum extends the analysis of Cron and Sherman <1> to incorporate an absorption loss and provides expressions for the noise power in an omnidirectional hydrophone, the noise level at the output of a conventional beamformer, and the spatial cross-correlation function. A comment is also made on the likely variation of noise level with frequency. These results are of use in assessing the performance of certain signal-processing techniques in high-frequency shallow-water ambient noise.

1 BASIC CONSIDERATIONS

The model generally used for low-frequency ambient noise based on theoretical considerations <1> and experimental data <2> is that the sea surface acts as a series of small independent noise sources radiating downwards into the sea. The level and radiation pattern of the sources are taken to be a function of wind speed, rainfall and frequency. Recent studies have incorporated acoustic interactions at the sea-bed <3,4>.

The small radiators are assumed to be close to the surface and to have an amplitude radiation pattern following $\cos^m\beta$, where β is the angle measured from the vertical and m , the surface noise directionality parameter, corresponds to whether the sources are monopole, dipole, etc. With m equal to zero, radiation is omnidirectional and the sources are monopoles; with m equal to 1, they represent dipoles produced by specular reflection in the sea surface. The dipole radiation pattern of $\cos\beta$ is, however, strictly applicable only to sources close to the surface in terms of the wavelength, as shown in Fig. 1.

At high frequencies (> 30 kHz), because acoustic bottom interactions are negligible, the propagation out to ranges of three times the water depth (β up to 70°) is reasonably well defined by straight-line paths. In consequence the propagation loss is given by $20 \log r + \alpha r$, where r is the slant range and α the absorption coefficient.

The use of a $\cos^m\beta$ amplitude radiation pattern at these frequencies may be questionable, since we are now dealing with small wavelengths (< 5 cm) and the formation of dipoles with a separation of much less than a wavelength is not possible. However, it is considered that some radiation pattern is applicable at moderate sea-states due to entrained air increasing the near-surface propagation loss. This radiation pattern may still be of the form $\cos^m\beta$, since for a given depth of entrained air the path length through the layer increases as $1/\cos\beta$ so that the noise amplitude below the layer may well vary as $\cos\beta$, see Fig. 2.

On the basis of the above, the geometry of the situation under consideration is given in Fig. 3, which shows a representative section of a small rectangular planar array located on the sea-bed with the water depth (z) being very much larger than the hydrophone spacing (s). The array is shown tilted by an angle γ to the horizontal along the q axis of the array.

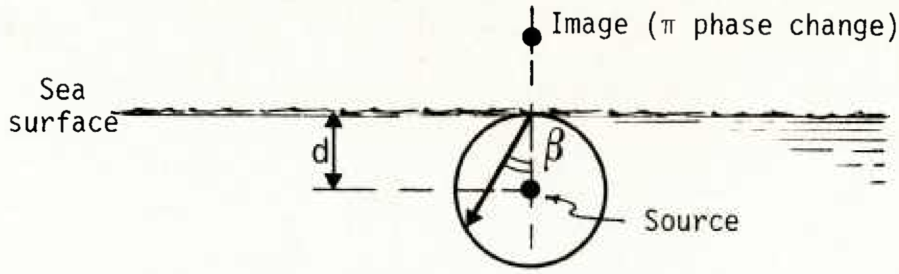

Radiation pattern $\propto \cos\beta$ if $d \ll \lambda$

FIG. 1 DIPOLE RADIATION PATTERN

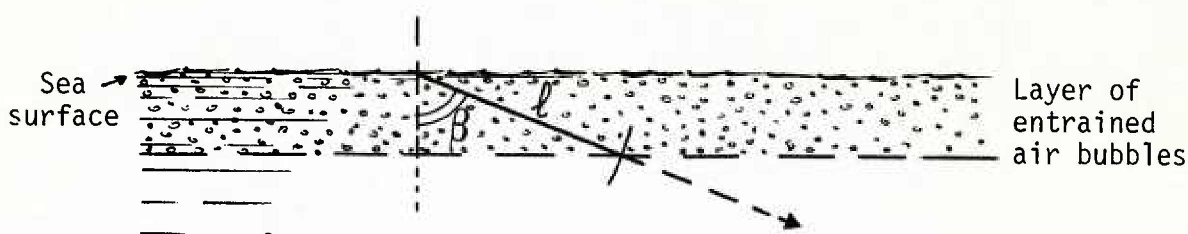

ℓ = $d/\cos\beta$ = path length through bubbles

Noise amplitude, in the far field of the source below the layer of bubbles $\propto \frac{1}{\ell} \propto \cos\beta$

FIG. 2 RADIATION THROUGH A LAYER OF BUBBLES

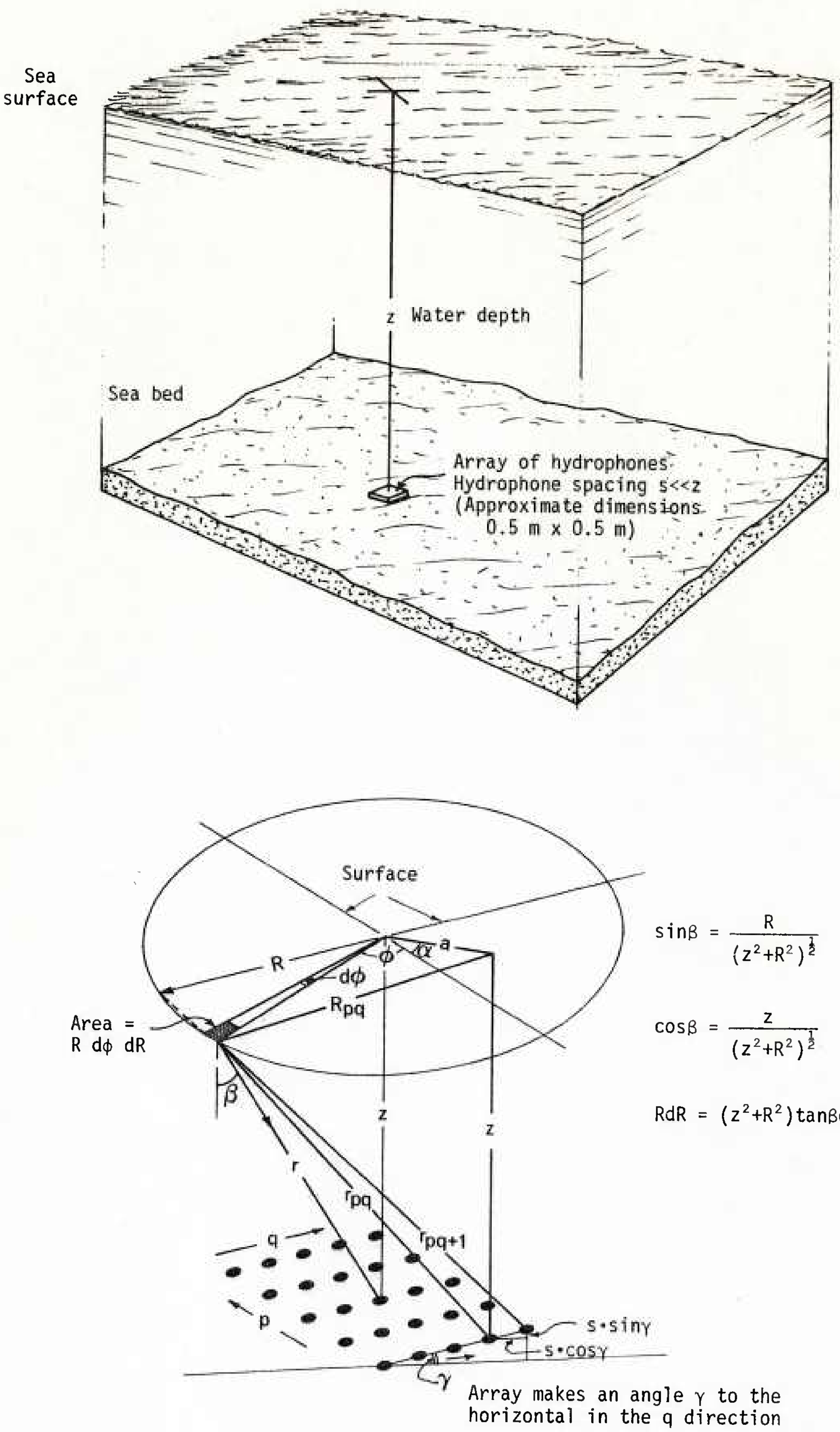

$$\sin\beta = \frac{R}{(z^2+R^2)^{\frac{1}{2}}}$$

$$\cos\beta = \frac{z}{(z^2+R^2)^{\frac{1}{2}}}$$

$$RdR = (z^2+R^2)\tan\beta d\beta$$

FIG. 3 GEOMETRY OF THE MODEL

2 NOISE LEVEL IN AN OMNIDIRECTIONAL HYDROPHONE

From Fig. 3 we have that the slant range r_{pq} from a small elemental area of the sea surface to the hydrophone in the pth row and the qth column of the array is given as follows:

$$r_{pq}^2 = (z - qs\cdot\sin\gamma)^2 + R_{pq}^2,$$

where

$$R_{pq}^2 = R^2 + p^2s^2 + q^2s^2\cdot\cos\gamma - 2R(p^2s^2 + q^2s^2\cdot\cos\gamma)^{\frac{1}{2}}\cos(\phi+\alpha).$$

Combining the above equations and using $(1+x)^{\frac{1}{2}} \cong 1+x/2$ if $x \ll 1$ we have

$$r_{pq} = (z^2+R^2)^{\frac{1}{2}}\left[1 + \frac{p^2s^2+q^2s^2}{2(z^2+R^2)} - \frac{zqs\cdot\sin\gamma}{(z^2+R^2)} - \frac{Rs}{(z^2+R^2)}(p\cdot\cos\phi - q\cdot\cos\gamma\cdot\sin\phi)\right]. \qquad \text{(Eq. 1)}$$

Thus we can obtain

$$r_{p,q+1} - r_{pq} = \frac{(1+2q)s^2}{2(z^2+R^2)^{\frac{1}{2}}} - \frac{zs\cdot\sin\gamma}{(z^2+R^2)^{\frac{1}{2}}} + \frac{Rs\cdot\cos\gamma\cdot\sin\phi}{(z^2+R^2)^{\frac{1}{2}}}.$$

Since $s^2 \ll z$, the first term can be dropped, giving:

$$r_{p,q+1} - r_{pq} = s\cdot\cos\gamma\cdot\sin\beta\cdot\sin\phi - s\cdot\sin\gamma\cdot\cos\beta. \qquad \text{(Eq. 1a)}$$

In a similar manner we can obtain

$$r_{p+1,q} - r_{pq} = -s\cdot\sin\beta\cdot\cos\phi. \qquad \text{(Eq. 1b)}$$

In the following it is assumed that the slant range (r) and the angle (β), as measured to the centre of the array, can be used to compute the noise amplitude at each hydrophone in the array. However, for noise phase the spacing of the hydrophones is taken into account.

At frequency f for the pq'th hydrophone, the noise signal amplitude in a 1 Hz band due to a unit area on the surface is given by:

$$n_{fpq} = \frac{n\cdot\cos^m\beta}{r}\, e^{-Ar}\cdot e^{-j(\omega t-kr)}, \qquad \text{(Eq. 2)}$$

where $n \cdot \cos^m\beta$ = noise signal radiated per unit area of the surface in a 1 Hz band,

A = absorption coefficient for signal amplitude expressed in exponential form,

k = wavenumber = $\frac{2\pi}{\lambda}$.

Then the noise power from the total surface is given by:

$$\overline{N^2_{fpq}} = E\left\{ \int_0^\infty \int_0^{2\pi} n_{fpq} \cdot n^*_{fpq} \, R \, d\phi \, dR \right\}, \qquad \text{(Eq. 2a)}$$

where E{ } denotes the expected value and the asterisk (*) indicates the complex conjugate. This gives, via Eq. 2 and Fig. 3,

$$\overline{N^2_{fpq}} = \overline{n^2}\pi \int_0^{\pi/2} \cos^{2m}\beta \cdot \tan\beta \cdot e^{-Az \cdot \sec\beta} \, d\beta, \qquad \text{(Eq. 2b)}$$

where $A = \alpha/4.343$, α being the absorption coefficient in dB/m.

Equation 2b can be readily integrated by using the substitution $\cos\beta = 1/t$, giving:

$$\overline{N^2_{fpq}} = \overline{n^2}\pi \, E_{2m+1}(AZ) \, , \qquad \text{(Eq. 2c)}$$

where E_k stands for the exponential integral of order k.

If the absorption loss is omitted, the exponential term in Eq. 2b would not be present and:

$$\overline{N^2_{fpq}}' \text{ (no absorption loss)} = \frac{\overline{n^2}\pi}{2m} \, . \qquad \text{(Eq. 2d)}$$

This suggests that at low frequencies, with no bottom interactions, the noise level in an omnidirectional hydrophone (Eq. 2d) is independent of the depth of the hydrophone. In our high-frequency case (Eq. 2c), the noise power is a function of depth and of absorption coefficient. Thus the high-frequency value of $\overline{N^2_{fpq}}$ has two components that vary with frequency: the value of $\overline{n^2}$, which for a given sea condition decreases with increasing frequency, and the exponential integral $E_{2m+1}(Az)$, which decreases with increasing frequency due to the increase in A.

Figure 4 plots values of $E_{2m+1}(Az)$ in decibels with respect to the level at 10 kHz for three typical shallow-water depths of 150, 300 and 450 m for frequencies from 10 to 100 kHz. The graphs are for values of m = 0 and m = 3, the extreme values. The value of m = 0 is likely to apply at low frequencies and for only small activity on the sea surface, that of m = 3 for high surface activity and high frequencies. Superimposed on these

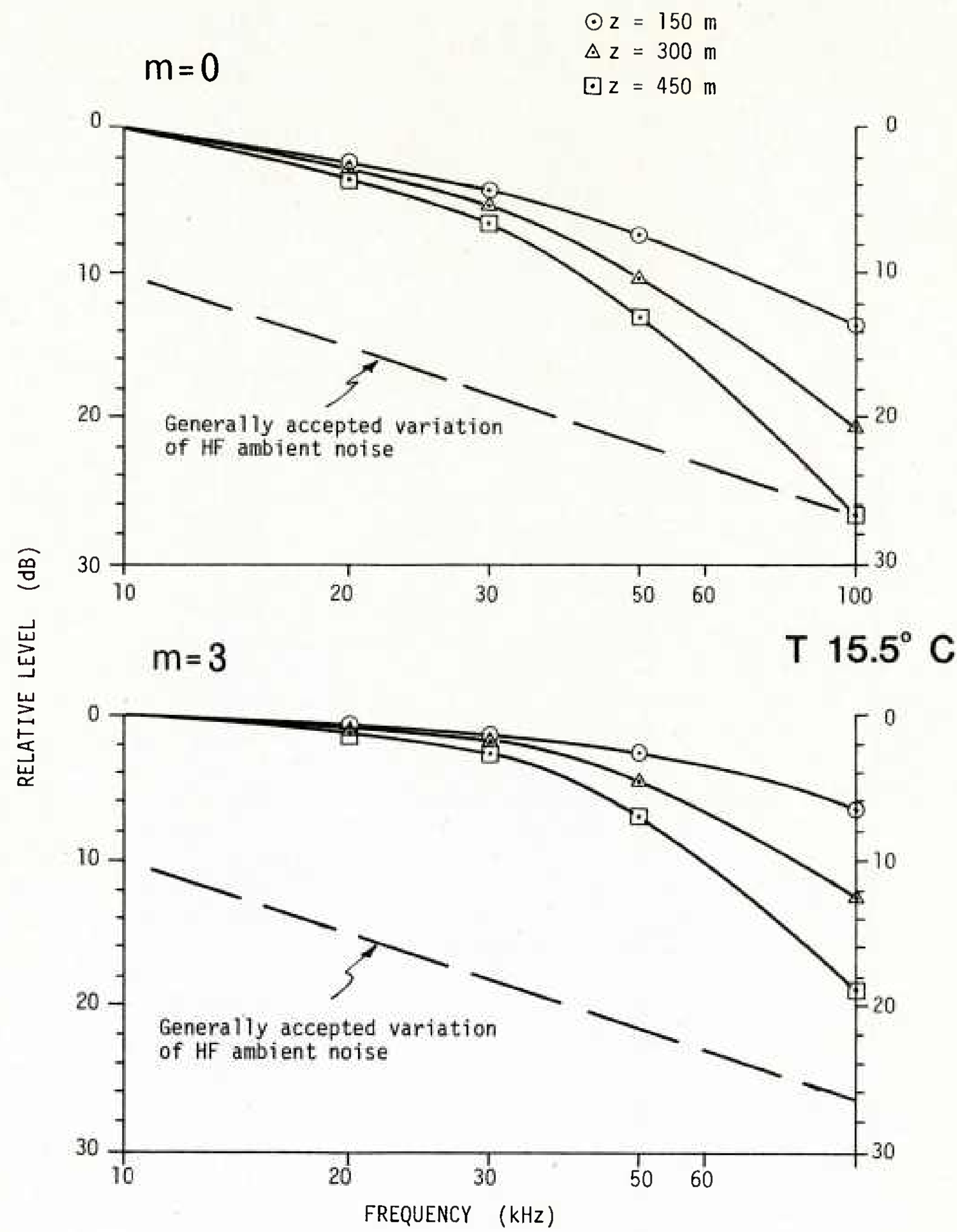

FIG. 4 VARIATION OF $E_{2m+1}(AZ)$ WITH FREQUENCY

graphs is a line showing the generally accepted slope for high-frequency ambient noise obtained by linear extrapolation from lower frequencies. It is seen that the $E_{2m+1}(Az)$ curves show a greater fall-off above 40 kHz than given by the linear extrapolation, particularly for low sea-state (m = 0) and the greater water depth (> 300 m). Because Eqs. 2c and 2d represent spectrum levels, the total noise power in a band form f_1 to f_2 is obtained by integrating over the band:

$$\overline{N^2_{Wpq}} = \int_{f_1}^{f_2} \overline{n^2}\, \pi\, E_{2m+1}(Az)df \;,$$

where band $W = f_2 - f_1$.

3 SPATIAL CORRELATION FUNCTION

For a single frequency (f) in our band of interest, the normalized spatial correlation function is given by:

$$\rho(x,f) = \frac{E\{n(f,x_1,y,z)\cdot n^*(f,x_2,y,z)\}}{\{E[n^2(f,x_1,y,z)]E\{n^2(f,x_2,y,z)]\}^{\frac{1}{2}},} \quad , \qquad \text{(Eq. 3)}$$

where E{ } refers to the expected value of the expression, n(f,x,y,z) represents the noise signal at frequency f and position (x,y,z), and it is assumed that the noise signals have zero mean values.

In terms of our geometry and model, and following the form of Eqs. 2 and 2a, Eq. 3 can be written as:

$$\rho(s,f) = \frac{1}{\overline{N^2_{fpq}}} \int_0^{\pi/2}\int_0^{2\pi} E\left\{n_{fpq}\cdot n^*_{fp,q+1}\right\} R\, d\phi\, d\beta, \qquad \text{(Eq. 3a)}$$

where $\overline{N^2_{fpq}}$ has been taken equal to $\overline{N^2_{fp,q+1}}$ on the basis of our earlier assumptions.

Thus the spatial correlation function for the noise from the total surface, following the form of Eqs. 2b and 2c, is given by:

$$\rho(s,f) = \frac{1}{\overline{N^2_{fpq}}} E\left\{\int_0^{\pi/2}\int_0^{2\pi} \frac{n^2 \cos^{2m}\beta}{2r^2} e^{-Ar} \cdot e^{jk(r_{p,q+1}-r_{pq})} R\, d\phi\, d\beta\right\}, \qquad \text{(Eq. 3b)}$$

which leads to

$$\rho(s,f) = \frac{\overline{n^2_{fpq}}}{2N^2_{fpq}} \int_0^{\pi/2} \cos^{2m-1}\beta \cdot \sin\beta \cdot e^{-Az\cdot\sec\beta} \int_0^{2\pi} \cos(ks\cdot\cos\gamma\cdot\sin\beta\cdot\sin\phi - ks\cdot\sin\gamma\cdot\cos\beta)\, d\phi\, d\beta.$$

In the integral over ϕ the integral of $\sin(ks\cdot\cos\gamma\cdot\sin\beta\cdot\sin\phi)$ is zero; thus we have:

$$\rho(s,f) = \frac{1}{E_{2m+1}(Az)} \int_0^{\pi/2} \cos^{2m-1}\beta\cdot\sin\beta\; e^{-Az\cdot\sec\beta} \cos(ks\cdot\cos\beta\cdot\sin\gamma) \cdot J_0(ks\cdot\cos\gamma\cdot\sin\beta)\, d\beta. \qquad \text{(Eq. 3c)}$$

A solution to this integral is given in Appendix A. For a horizontal separation ($\gamma = 0$), the following expression obtains:

$$\rho(x,f) = \frac{1}{E_{2m+1}(Az)} \sum_{\mu=0}^{\infty} \frac{(\tfrac{1}{2}ks)^{\mu}}{\mu!} J_{\mu}(ks) E_{2m+1+2\mu}(Az)\,, \qquad \text{(Eq. 3d)}$$

where k = wavenumber and s = hydrophone spacing.

For a vertical separation ($\gamma = 90°$) we have:

$$\rho(z,f) = \frac{1}{E_{2m+1}(Az)} \sum_{i=0}^{\infty} \frac{(-k^2s^2)^{i}}{(2i)!} E_{2m+1+2i}(Az). \qquad \text{(Eq. 3e)}$$

The corresponding equations by Cron and Sherman <1> for the case when absorption loss is neglected are

$$\rho'(x) = \frac{2^m m!\; J_m(ks)}{(ks)^m}\,, \qquad \text{(Eq. 3f)}$$

$$\rho'(z) = 2m \int_0^1 X^{2m-1} \cos(ksX)\, dX. \qquad \text{(Eq. 3g)}$$

As can be seen from Appendix A, it is not easy to show directly that when A is set equal to zero Eqs. 3d and 3e are the same as Eqs. 3f and 3g respectively. However, it can be shown indirectly by comparing the numerical values obtained from the two pairs of equations.

This comparison is done for different values of m in Fig. 5 for $\rho(x)$ and in Fig. 6 for $\rho(z)$, where the solid line represents the values from the present analysis with a very small value of A (A is set equal to 0.0001, which represents 0.43 dB/km), and the dashed lines represent the values from Cron and Sherman <1>.

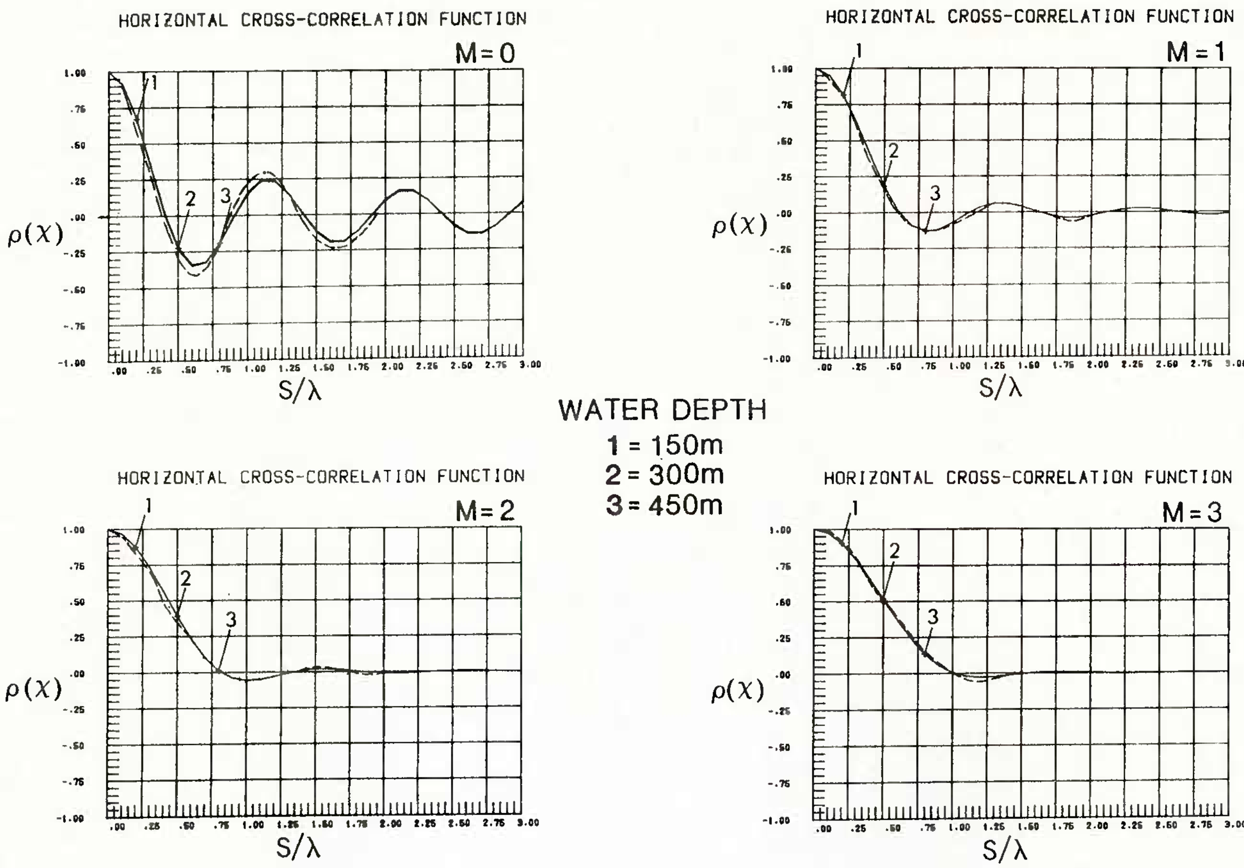

FIG. 5 COMPARISON OF ρ(x) WITH LOW FREQUENCY ANALYSIS

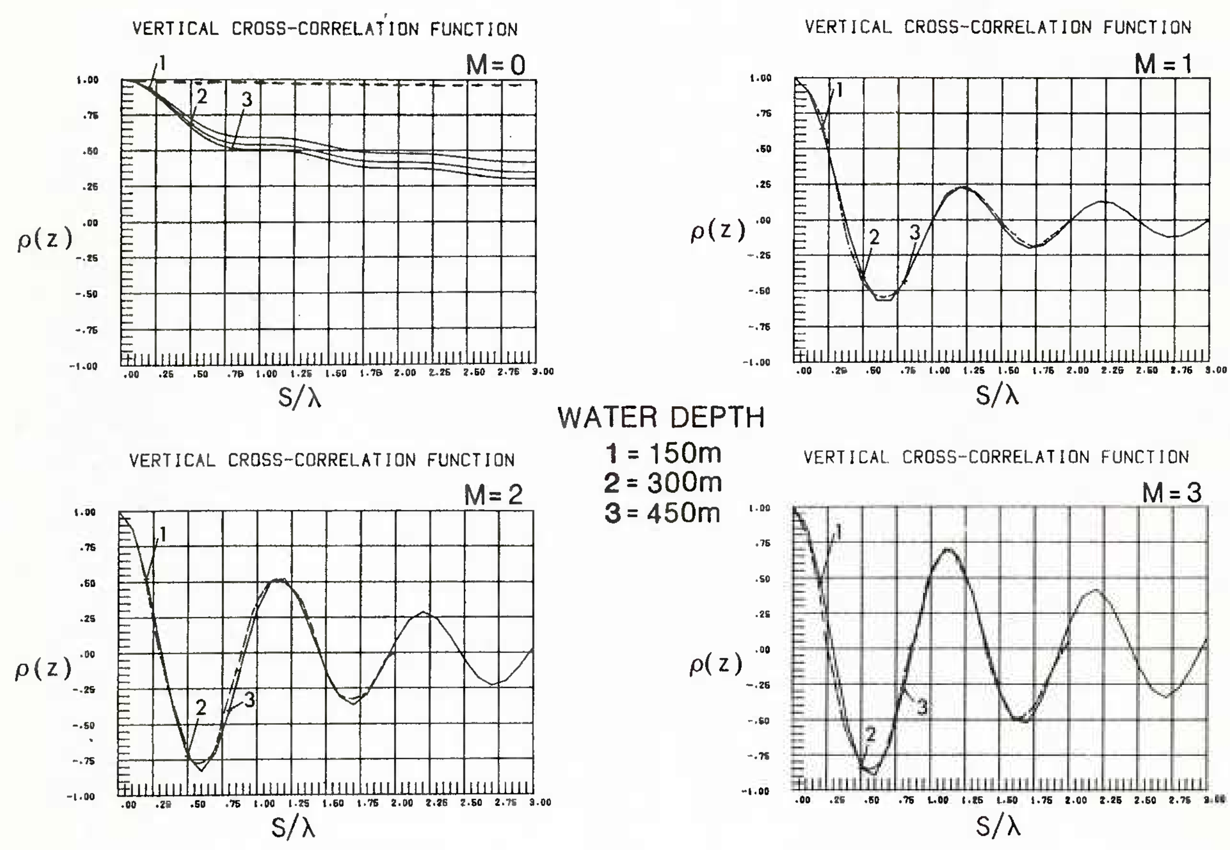

FIG. 6 COMPARISON OF ρ(z) WITH LOW FREQUENCY ANALYSIS

It is seen that good agreement exists with $\rho'(x)$ for all values of m, and also with $\rho'(z)$ except for the case of m equal to zero. In this instance, it is seen that the Cron & Sherman expression gives a value of 1 for $\rho(z)$, independent of the normalized element spacing s/λ, whereas when an absorption loss is included the present analysis gives a reducing value of $\rho(z)$ as s/λ is increased. As will be seen in the next figures, the value of $\rho(z)$ becomes oscillatory about zero for m equal to zero when the absorption loss is greater than a value corresponding to 20 kHz and for water depths greater than 150 m.

Value of $\rho(x)$ and $\rho(z)$ are plotted in Figs. 7a, 7b, 7c and 7d and in Figs. 8a, 8b, 8c and 8d respectively. The graphs are for the three sample depths of 150, 300 and 450 m, frequencies of 20, 50 and 100 kHz, and m equal to 0, 1, 2 and 3.

The effects of the three variables of m, frequency, and water depth shown by Figs. 7 and 8 are plausible and consistent with the previous deep-water low-frequency analyses <1,2,3>. The values of s/λ at which $\rho(x)$ and $\rho(z)$ have their first zeros are, for m equal to 1, a water depth of 450 m, and a frequency of 20 kHz, 0.6 and 0.3 respectively; the values at low frequency <1,2,3> are 0.6 and 0.35, see Figs. 5 and 6. The effect on $\rho(z)$ and $\rho(z)$ of increasing m, that is of making the field more directional, is also consistent with the low-frequency values. Increasing the water depth will increase the propagation loss from the surface along a given angle of incidence at the sea bed, which will make the field more directional and thus have a similar effect to increasing m. A similar argument applies to an increase in frequency (increases in absorption coefficient). In summary, therefore, the curve for $\rho(x)$ is effectively stretched out by an increase in m, water depth, or frequency, whereas the opposite applies to $\rho(z)$.

4 NOISE LEVEL IN A BEAM

The analysis given above can be extended to give the noise power in a beam produced by a conventional beamformer, that is, a beam formed by summing the phase-shifted, but unweighted, hydrophone outputs.

The array, with dimensions small compared with the water depth, is assumed to be tilted at an angle γ to the horizontal in the q direction, and the steering is taken to be along the q axis only, so that the beam is steered in the same plane as the array is tilted. The beamforming can thus be represented either by summing along the q axis after the appropriate delays and then summing across p, or by summing across p without steer delays and then summing along q with the appropriate delays. The first sequence will be used in the following.

Let the steer angle measured from the vertical be θ, then the phase shifts required along the q axis are $qk \cdot \sin\theta$, where q varies from $-(Q-1)/2$ to $+(Q-1)/2$ or from 0 to $Q-1$.

For the wavefront of the noise from a small elemental area of the sea surface a reference time is taken at one end of the array (the 'zero' end

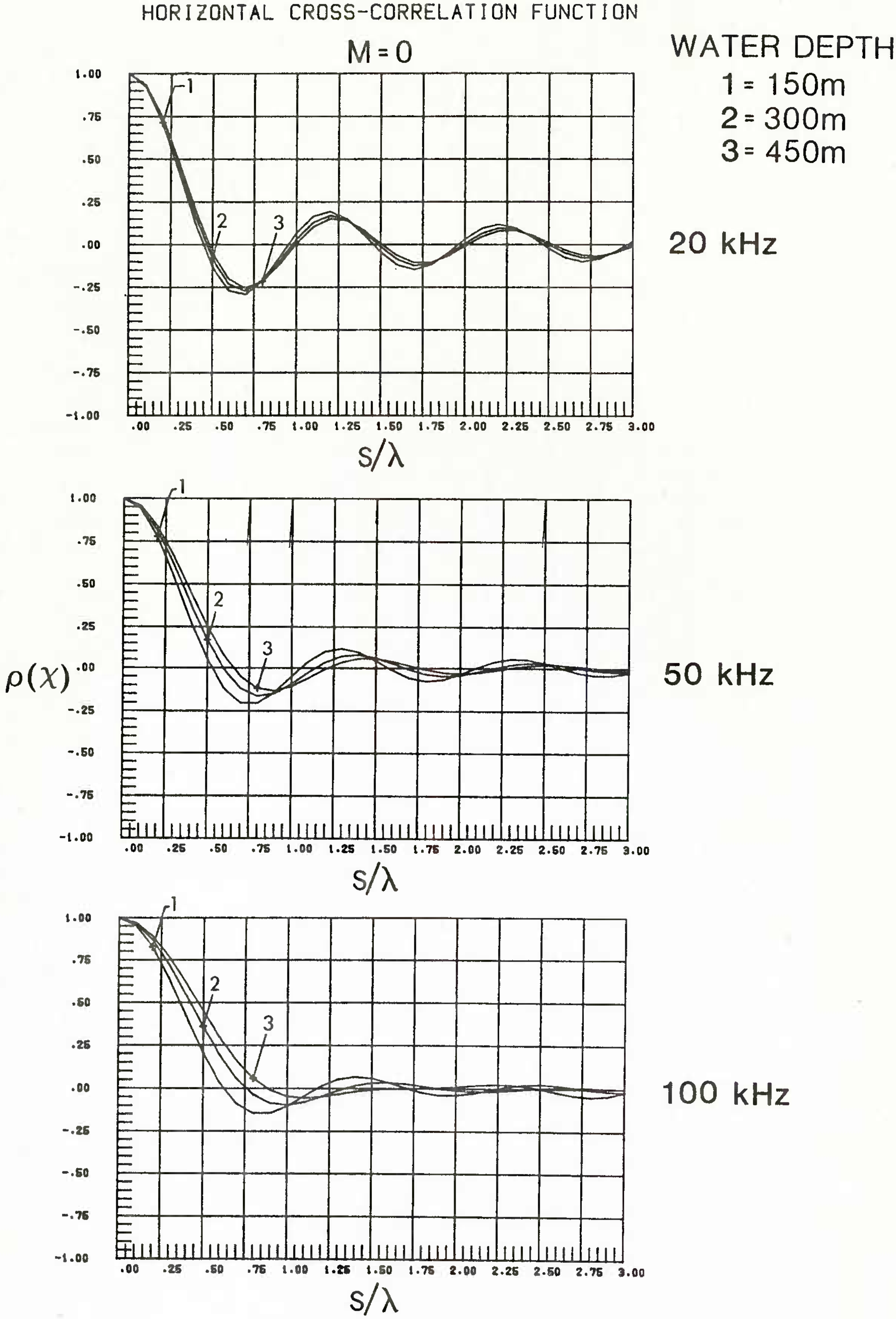

FIG. 7a HORIZONTAL CROSS-CORRELATION FUNCTION (M = 0)

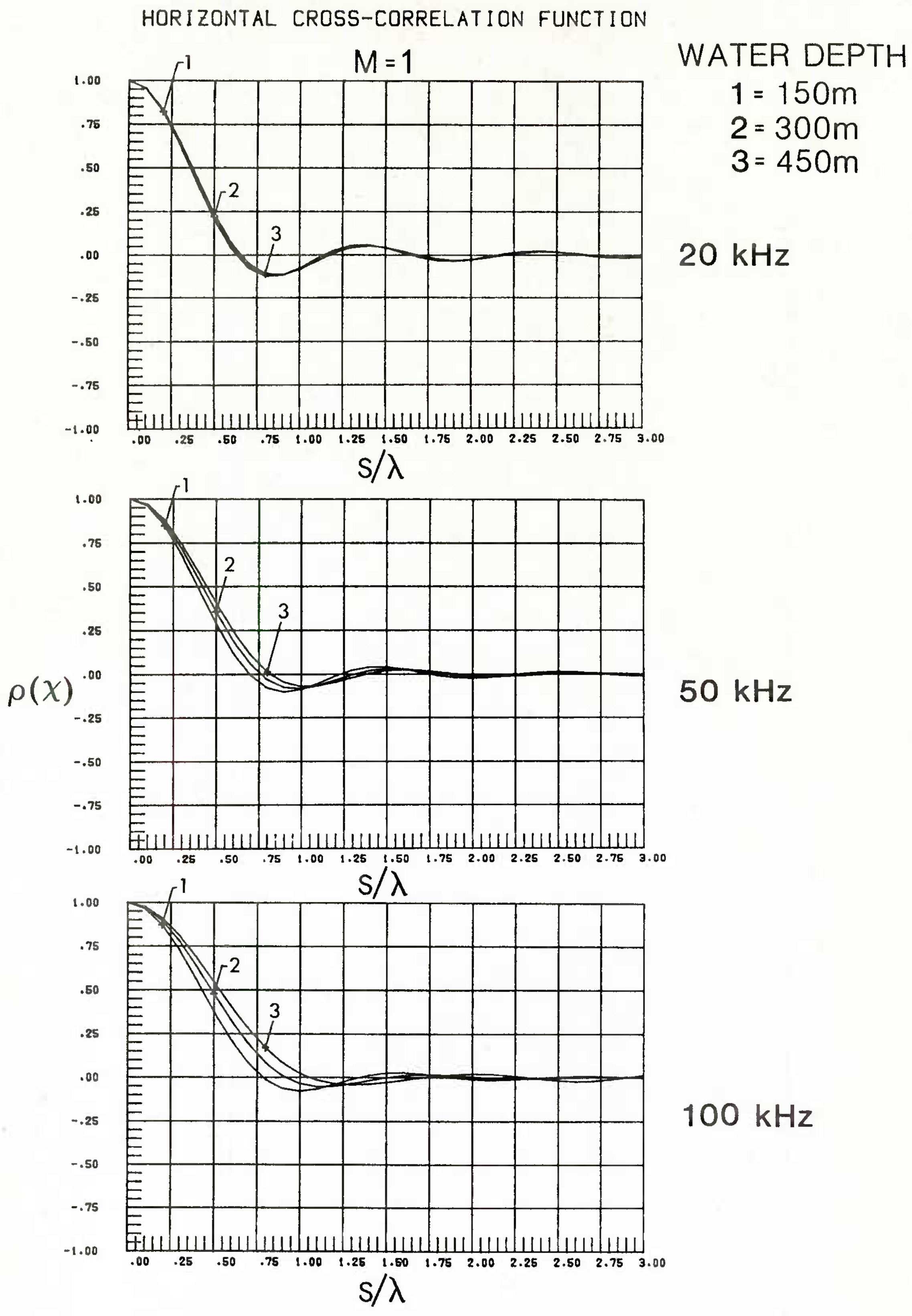

FIG. 7b HORIZONTAL CROSS-CORRELATION FUNCTION (M = 1)

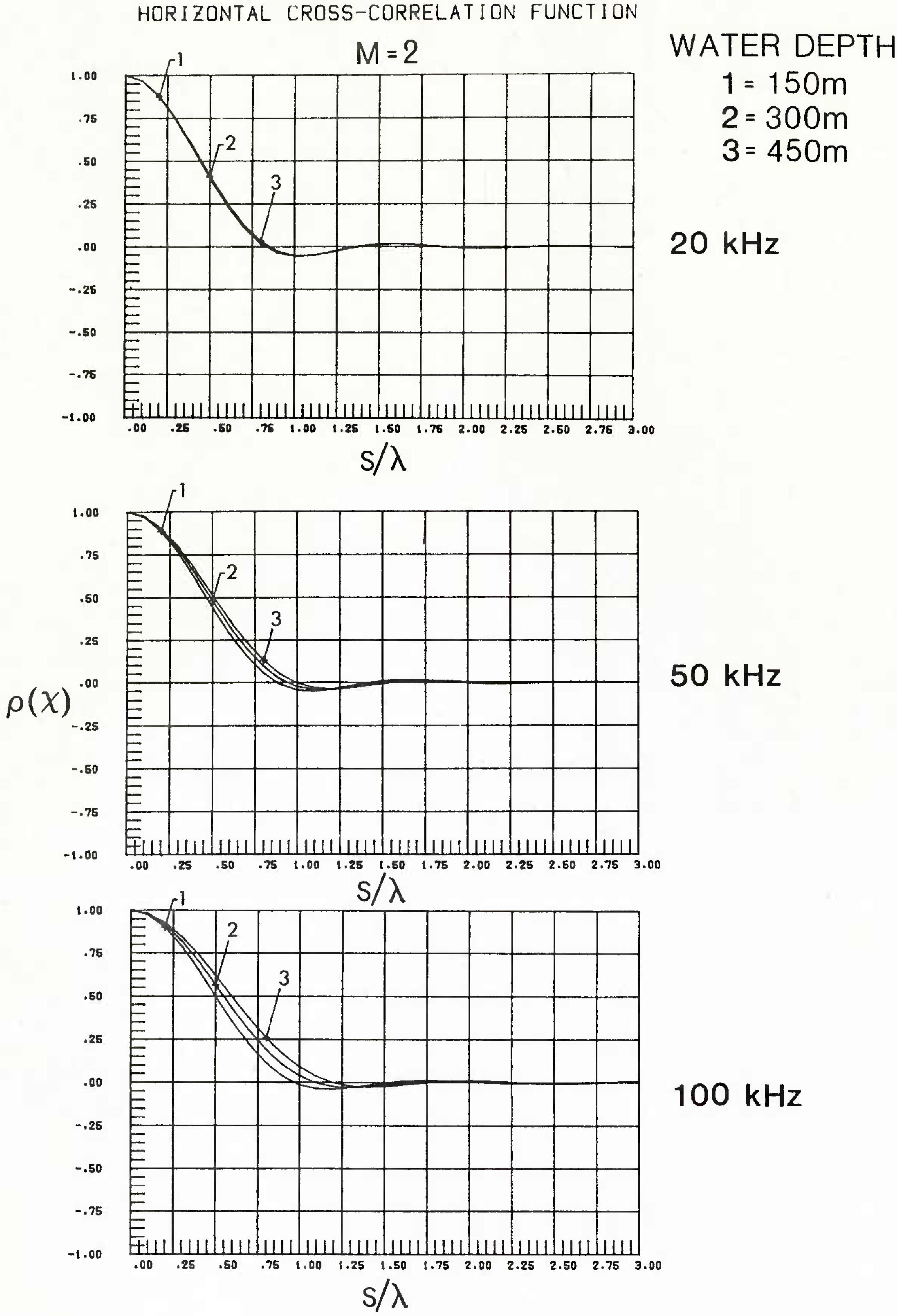

FIG. 7c HORIZONTAL CROSS-CORRELATION FUNCTION (M = 2)

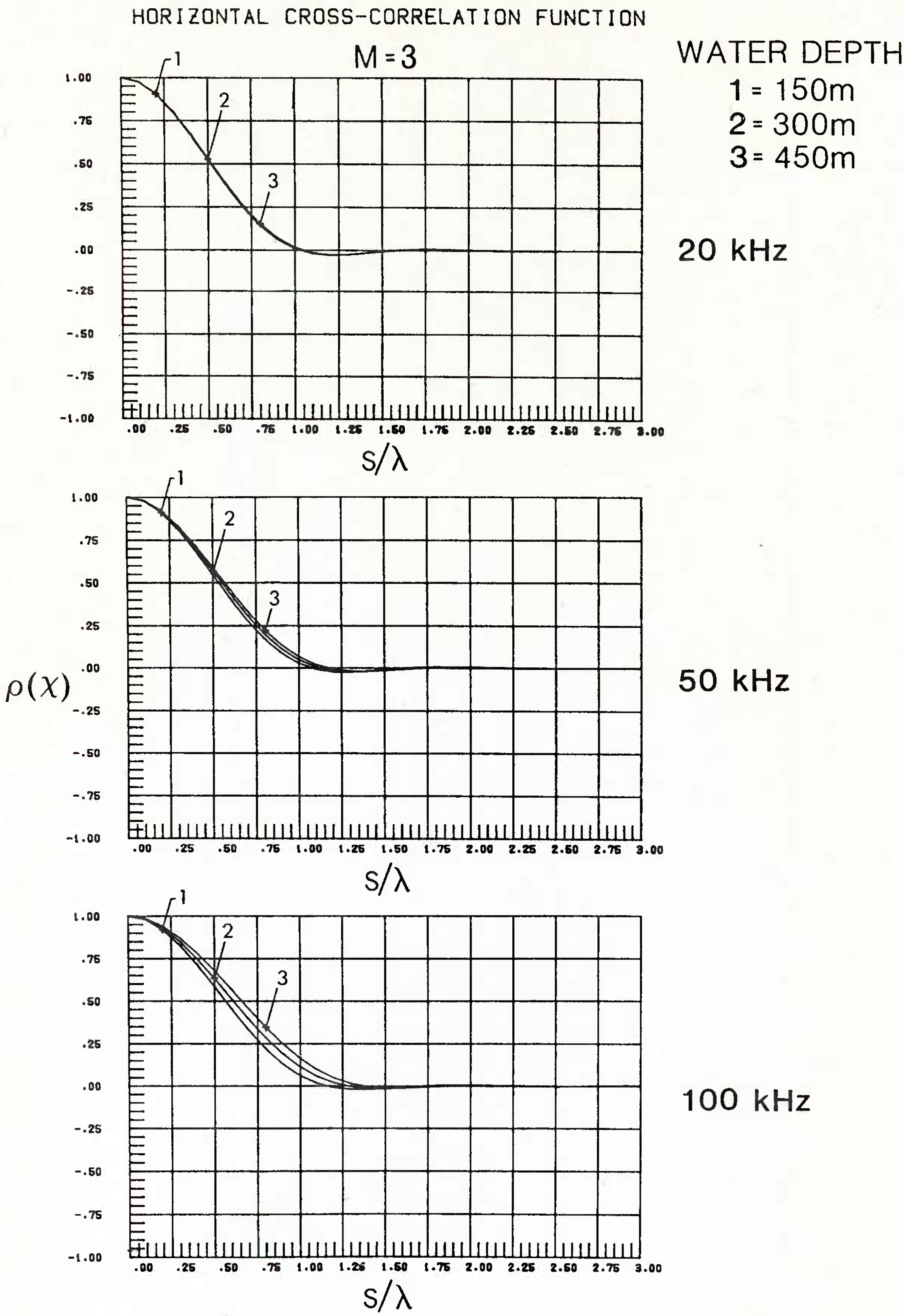

FIG. 7d HORIZONTAL CROSS-CORRELATION FUNCTION (M = 3)

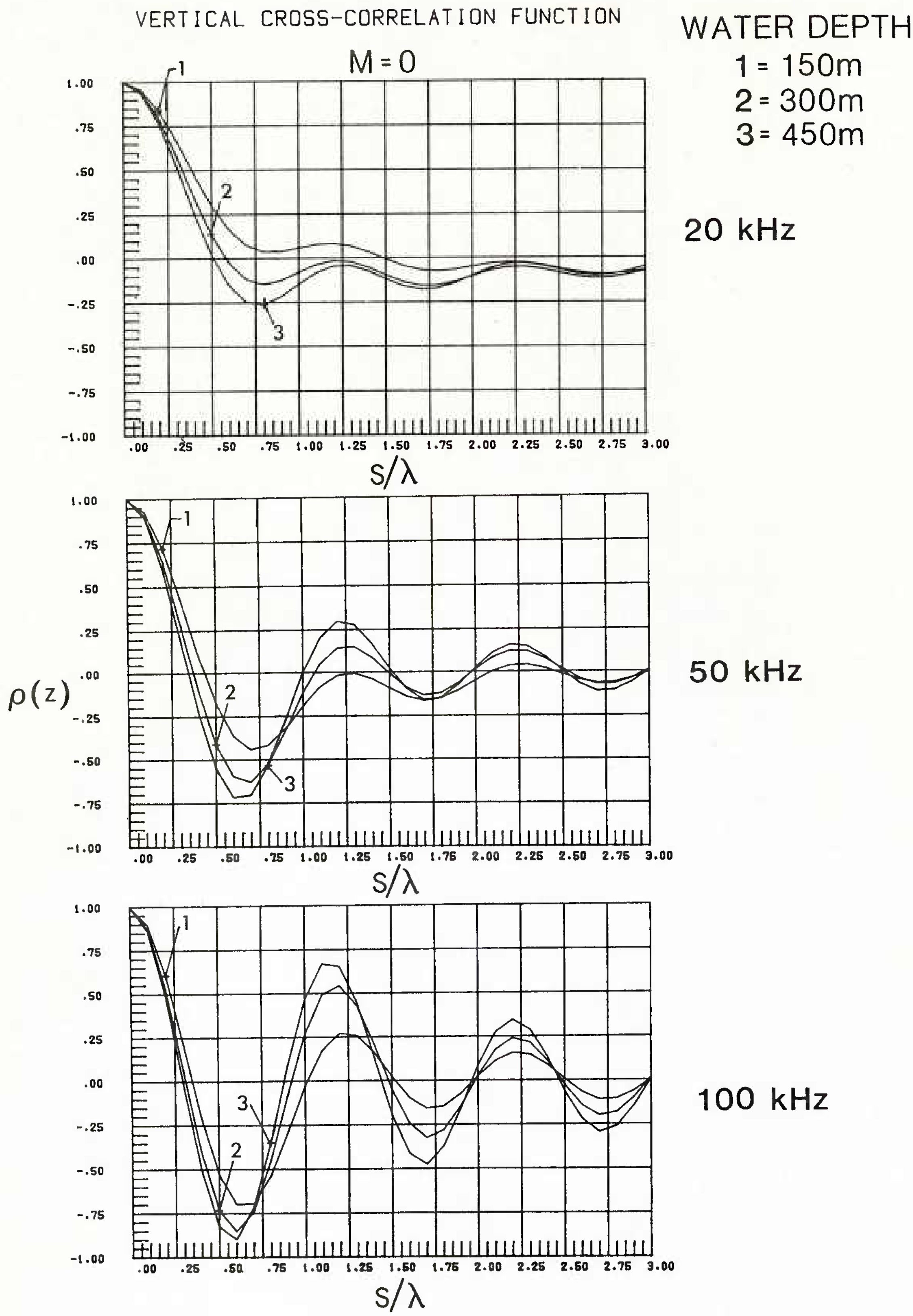

FIG. 8a VERTICAL CROSS-CORRELATION FUNCTION (M = O)

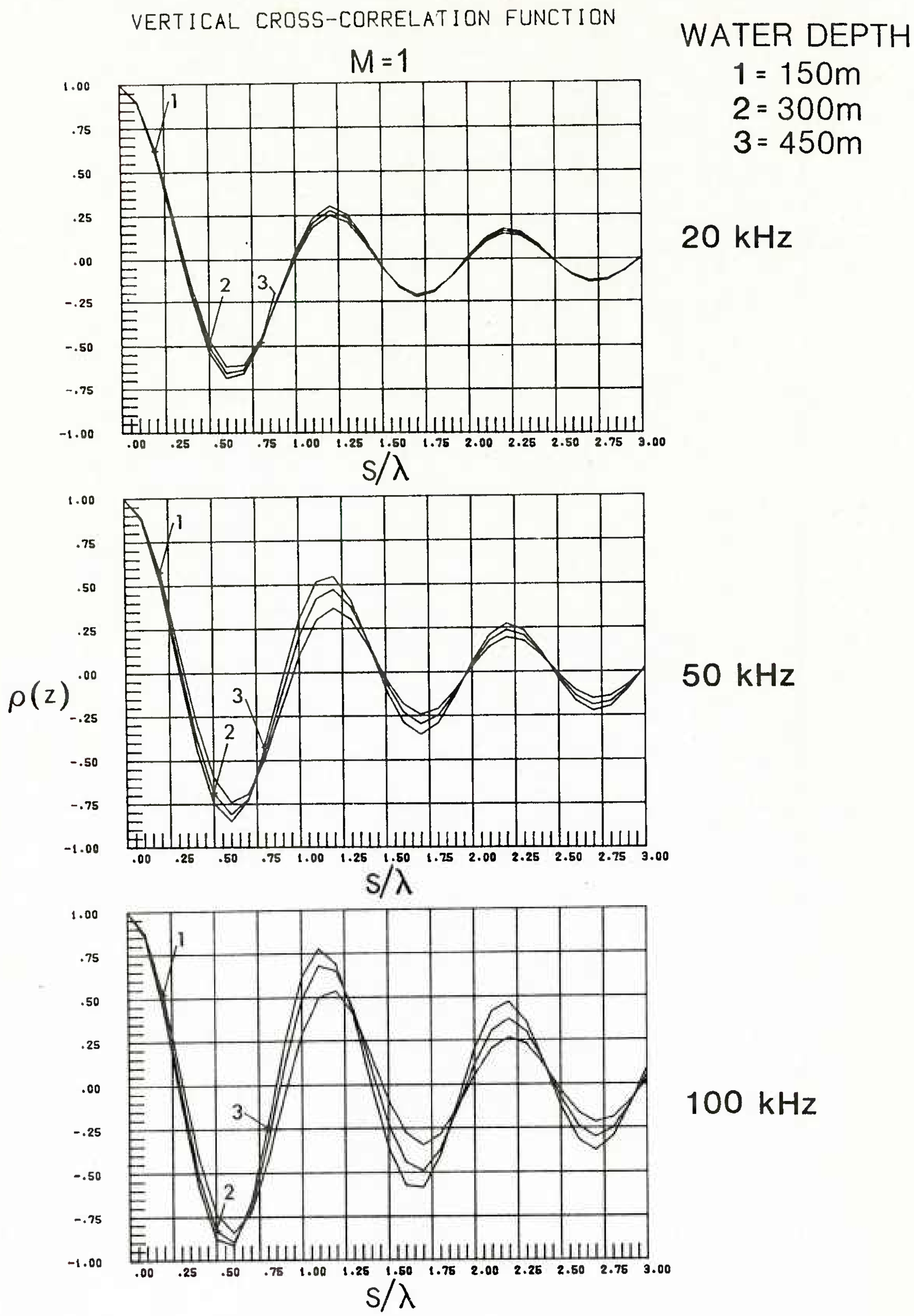

FIG. 8b VERTICAL CROSS-CORRELATION FUNCTION (M = 1)

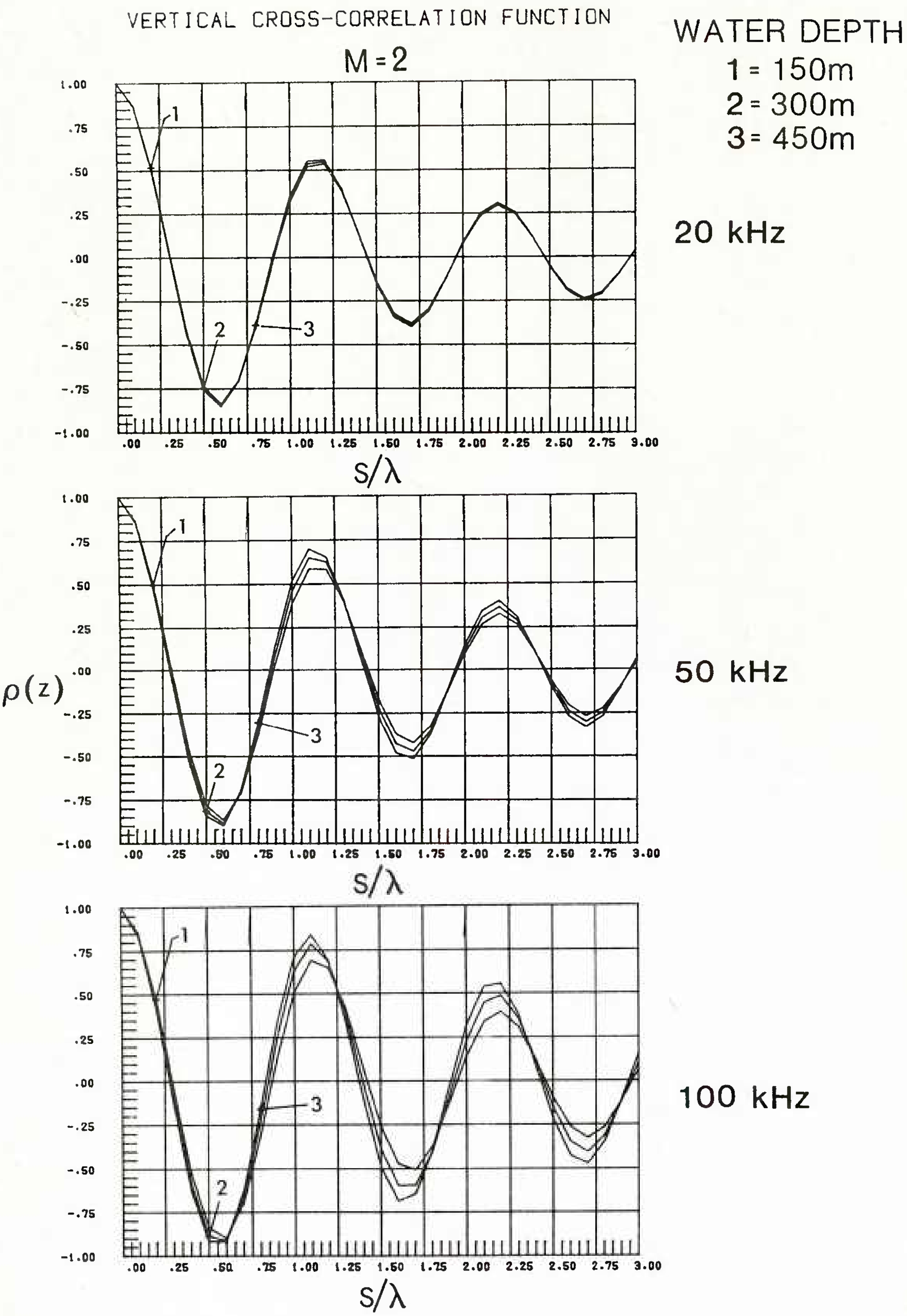

FIG. 8c VERTICAL CROSS-CORRELATION FUNCTION (M = 2)

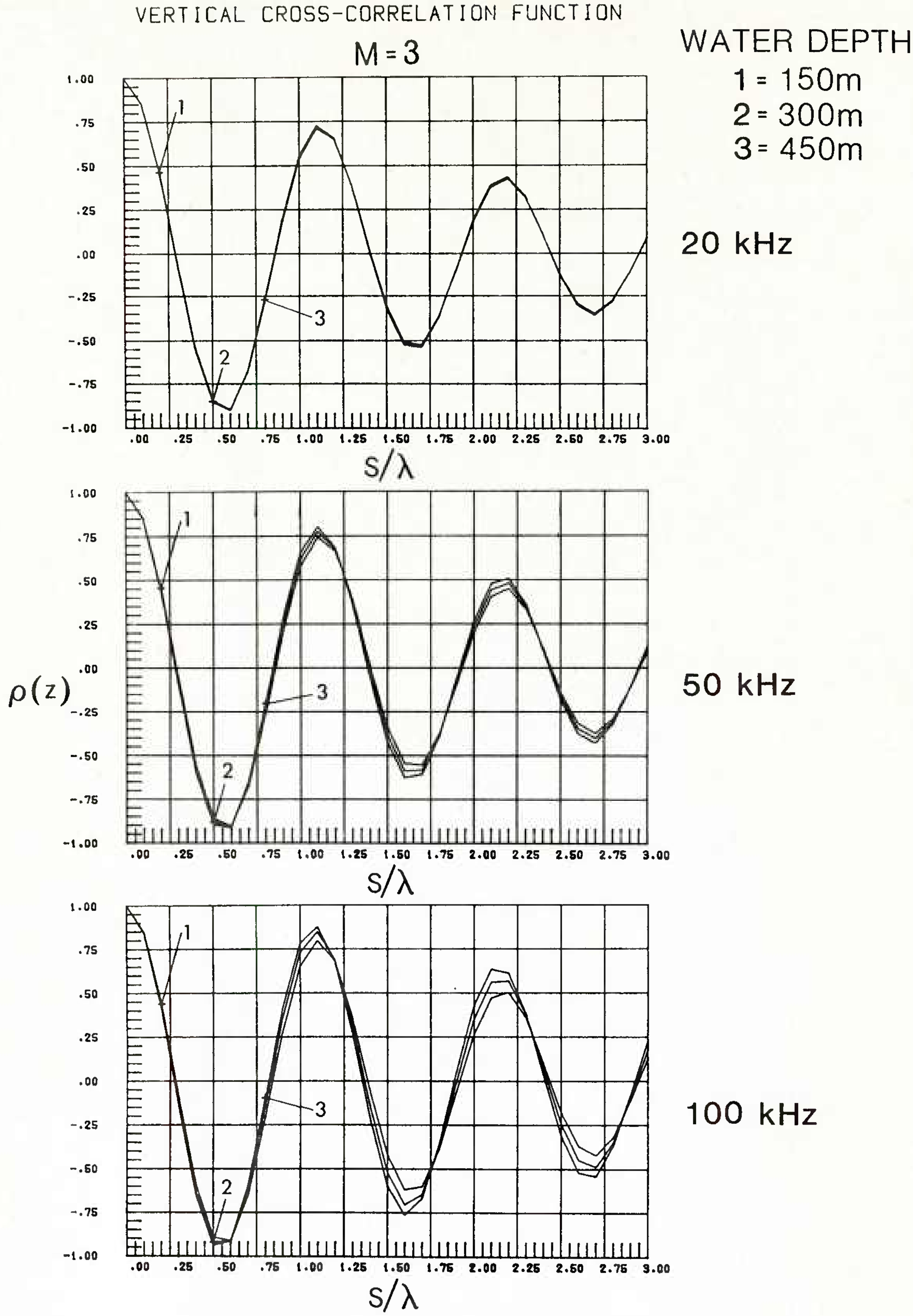

FIG. 8d VERTICAL CROSS-CORRELATION FUNCTION (M = 3)

in the above summation). Thus the incremental delays of the wavefront along the q axis can be obtained from the increment in the slant range (r_{pq}) along the q axis, i.e. by $r_{p,q+1} - r_{pq}$.

The noise amplitude along the q axis in the pth column due to a small elemental area of the surface is then:

$$N_q(\theta) = \frac{n \cdot \cos^m\beta}{r} \, e^{-j\omega t} \sum_{q=0}^{Q-1} e^{-jqk \cdot \sin\theta} \, e^{-jq(r_{p,q+1} - r_{pq})} \, e^{-AR} \, ,$$

with the value of β, and that of r associated with noise amplitude, taken as independent of p or q since the array dimensions are small compared with the water depth.

The sum of $N_q(\theta)$ across the p axis can similarly be obtained by taking increments of $r_{p+1,q} - r_{pq}$. From Eqs. 1a and 1b, we have

$$r_{p,q+1} - r_{pq} = s(\cos\gamma \cdot \sin\beta \cdot \sin\phi - \sin\gamma \cdot \cos\beta)$$

and

$$r_{p+1,q} - r_{pq} = -s \cdot \sin\beta \cdot \cos\phi .$$

Then the total noise amplitude across the full array is given by:

$$N_{pq}(\theta) = \sum_{p=0}^{P-1} e^{-jpks \cdot \sin\beta \cdot \cos\phi} \, N_q(\theta) \, . \qquad \text{(Eq. 4)}$$

That is:

$$N_{pq}(\theta) = n \cos^m\beta \, \frac{e}{r}^{-j\omega t - Ar} \sum_{p=0}^{P-1} e^{-jpks \cdot \sin\beta \cdot \cos\phi}$$

$$\sum_{q=0}^{Q-1} e^{-jks(\sin\beta \cdot \cos\gamma \cdot \sin\phi - \sin\gamma \cdot \cos\beta)} \, e^{-jks \cdot \sin\theta} \qquad \text{(Eq. 4a)}$$

$$= n \cos^m\beta \cdot \frac{e}{r}^{-j\omega t - Ar} \sum_{p=0}^{P-1} e^{-jpx} \sum_{q=0}^{Q-1} e^{-jqy} \, , \qquad \text{(Eq. 4b)}$$

where

$$x = ks \cdot \sin\beta \cdot \cos\phi$$

and

$$y = ks(\sin\beta \cdot \cos\gamma \cdot \sin\phi - \sin\gamma \cdot \cos\beta + \sin\theta).$$

Since

$$\sum_{p=0}^{P-1} e^{-jpx} = e^{-j\frac{x}{2}(P-1)} \frac{\sin\frac{Px}{2}}{\sin\frac{x}{2}} , \qquad \text{(Eq. 4c)}$$

$$\sum_{q=0}^{Q-1} e^{-jqy} = e^{-j\frac{y}{2}(Q-1)} \frac{\sin\frac{Qy}{2}}{\sin\frac{y}{2}} \qquad \text{(Eq. 4d)}$$

Thus we have:

$$N_{pq}(\theta) = n\cdot\cos^{m}\beta\, \frac{e}{r}^{\,jwt-Ar}\, e^{-j\frac{x}{2}(P-1)} \frac{\sin\frac{Px}{2}}{\sin\frac{x}{2}}\; e^{-j\frac{y}{2}(Q-1)} \frac{\sin\frac{Qy}{2}}{\sin\frac{y}{2}} .$$

The total noise power in the beam is then given by:

$$\overline{N^2}(\theta) = E \int_0^{\infty}\int_0^{2\pi} N_{pq}(\theta)\cdot N^*_{pq}(\theta) R\, d\phi\, dR$$

$$= \overline{n^2}\, P^2Q^2 \int_0^{\pi/2}\int_0^{2\pi} \cos^{2m-1}\beta\, \sin\beta\cdot e^{-Az\cdot\sec\beta}\, [f(P)\cdot F(Q)]^2\, d\phi\, d\beta ,$$

(Eq. 4e)

where $f(P) = \dfrac{\sin(\frac{1}{2}Pks\cdot\sin\beta\cdot\cos\phi)}{P\sin(\frac{1}{2}ks\cdot\sin\beta\cdot\cos\phi)}$

and $F(Q) = \dfrac{\sin[\frac{1}{2}Qks(\sin\beta\cdot\cos\gamma\cdot\sin\phi - \sin\gamma\cdot\cos\beta + \sin\theta)]}{Q\cdot\sin[\frac{1}{2}ks(\sin\beta\cdot\cos\gamma\cdot\sin\phi - \sin\gamma\cdot\cos\beta + \sin\theta)]}$

Equation 4e is evaluated in Appendix B to give

$$\overline{N^2}(\theta) = \frac{2\pi n^2}{P^2Q^2} \sum_{i=0}^{\infty} \sum_{n=0}^{\infty} \sum_{r=0}^{P-1} \sum_{t=0}^{Q-1} A_r B_t (-)^i \frac{(\lambda/2)^n\, J_n(\lambda)}{n!}$$

$$\frac{\cos p\cdot q^{2i}}{(2i)!} E_{2m+2n+2i+1}(Az) + \frac{\sin p\cdot q^{2i+1}}{(2i+1)!} E_{2m+2n+2i+2}(Az),$$

where

$A_o = P \qquad B_o = Q$

$A_r = 2(P-r) \quad (r > 0) \qquad B_t = 2(Q-t) \quad (t > 0)$

$\lambda = ks\sqrt{r^2+t^2\cos^2\gamma} \qquad p = kst\cdot\sin\theta \qquad q = kst\cdot\sin\gamma$

This is a fairly complex expression and, of course, applies only to an unshaded array. A closed-form solution for a shaded array would be achievable if the shading functions allow summations to be made, as in Eqs. 4c and 4d. If the shading function is known, then the total power in a beam is probably best evaluated using numerical integration.

For a horizontal array, in which $\gamma = 0$, Eq. 4f becomes

$$\overline{N^2}(\theta)_H = \frac{2\pi\overline{n^2}}{P^2Q^2} \sum_{n=0}^{\infty} \sum_{r=0}^{P-1} \sum_{t=0}^{Q-1} A_r B_t \cos P \frac{(\lambda_1/2)^n}{n!} J_n(\lambda_1) E_{2m+2n+1}(Az), \qquad \text{(Eq. 4g)}$$

where $\lambda_1 = ks\sqrt{r^2+t^2}$,

$p = kst \cdot \sin\theta$.

In the case of a vertical array, in which $\gamma = \pi/2$, the quadruple summation remains as in Eq. 4f, but now

$\lambda_2 = ksr \qquad q = kst$

and there are only P terms of the form $\dfrac{(\lambda_2/2)^n}{n!} J_n(\lambda_2)$.

CONCLUSIONS AND RECOMMENDATIONS

If the model of high-frequency ambient noise in shallow water proposed and examined in this study is reasonable, then:

a. Care should be taken in using noise levels obtained by linear extrapolation from the lower frequencies. The study suggests that the noise power in an omnidirectional hydrophone (Eq. 2c and Fig. 3) falls off more rapidly with frequency above 40 kHz, particularly for low sea states (m equal to zero) and for greater water depth (z = 150 m), than is predicted by linear extrapolation from the lower frequencies.

b. When designing an array for use near the sea bed at frequencies above 20 kHz, the value of hydrophone separation for the first zero in $\rho(x)$ or $\rho(z)$ may be a function of sea state, frequency, and water depth. From the results in Figs. 7 and 8 it would appear necessary to space the elements by more than $\lambda/2$ for horizontal arrays and less than $\lambda/2$ for vertical arrays, depending on the value of m that is applicable, the frequency in use, and the water depth. For example, for m equal to 1, a frequency of 50 kHz, and a water depth of 300 m, the optimum spacing for a horizontal array is 0.75λ and a vertical array 0.3λ.

c. The expression for the total ambient noise power in an unshaded array is complex (see Eqs. 4f, 4g and 4h). For a shaded array, it is possible to obtain a closed-form solution only for those shading functions that allow the summations in Eqs. 4c and 4d. For other shading functions, however, a solution could be obtained using numerical integration.

Experimental data are required to verify the model and the resulting analysis. Measurements are proposed as follows:

1) Noise Levels

The noise level in an omnidirectional hydrophone placed on or near the sea-bed should be measured as a function of sea-state (wind speed), frequency, and water depth for comparison with Eq. 2c and Fig. 3 and to give estimates of the value of n^2.

2) Noise Directionality

Measurements should be made of the high-frequency noise level in shallow water using a high-resolution array (narrow mainlobe and low sidelobe levels). The array should be situated on or near the sea-bed and capable of being tilted to various angles away from the vertical. Preferably, for a given sea-state, simultaneous measurements should be made at two different depression angles e.g. one array at zero depression (looking vertical), the other at 30° depression. A sampling technique could be developed to measure the noise levels for a given sea-state over the whole vertical arc; for example, with two arrays, sample vertically and at 30° depression for 5 minutes, then at 10° and 40° for 5 minutes, then at 20° and 50°, etc.

3) Spatial Correlation

It is recommended that consideration be given to the construction of a device to measure $\rho(x)$ and $\rho(z)$ over the frequency range of 30 to 100 kHz. This would require the use of very small ball hydrophones, say 0.2 cm diameter, spaced on horizontal and vertical axes in such a manner as to provide adequate samples of $\rho(x)$ and $\rho(z)$ out to values of $s/\lambda = 2$. This could be done with 24 hydrophones (12 on each axis) with a separation of 0.5 cm (0.167λ).

4) Noise Power in a Beam

It is recommended that the outputs of the small hydrophones outlined above be summed to form simple, unsteered beams, with or without shading, to provide experimental results for comparison with Eqs. 4g and 4h. The elements could be tilted to evaluate the effect of γ, the tilt angle.

ACKNOWLEDGMENTS

The following members of SACLANTCEN contributed to the work reported in this document.

Signal Processing Group	S. Bongi	Computer programming
Consultant	A. Nuttall	Comments and advice

REFERENCES

1. CRON, B.F. and SHERMAN, C.H. Spatial correlation functions for various noise models. Journal Acoustical Society of America, 34, 1962: 1732-1736.

2. COX, H. Spatial correlation in arbitrary noise fields with application to ambient sea noise. Journal Acoustical Society of America 54, 1973: 1289-1301.

3. KUPERMAN, W.A. and INGENITO, F. Spatial correlation of surface-generated noise in a stratified ocean. Journal Acoustical Society of America 67, 1980: 1988-1996.

4. BUCKINGHAM, M.J. Spatial coherence of wind-generated noise in a shallow ocean channel. Journal Acoustical Society of America, 70, 1981: 1412-1420.

5. LINETTE, H.M. and RORY, J.T. Directivity study of the noise field in the ocean, employing a correlative dipole. Journal Acoustical Society of America 36, 1964: 1788-1794.

6. ARASE, E.M. and ARASE, T. Correlation of ambient sea noise. Journal of Acoustical Society of America 40, 1966: 205-210.

APPENDICES

APPENDIX A

EVALUATION OF THE BESSEL TRIGONOMETRIC INTEGRAL FOR THE SPATIAL CROSS-CORRELATION FUNCTION

In Eq. 3c of the main text, the spatial cross-correlation function includes the integral

$$I_1 = \int_0^{\pi/2} \cos^{2m-1}\beta\cdot\sin\beta\cdot\exp(-Az\ \sec\beta)\cos(ks\cdot\cos\beta\cdot\sin\gamma)J_o(ks\cdot\cos\gamma\cdot\sin\beta)\ d\beta, \qquad \text{(Eq. A.1)}$$

where m is a positive integer, and Az is a positive constant.

As this integral does not seem to have been evaluated before (since it does not appear in collections of integrals such as <A.1>, the development of a form suitable for numerical calculations is presented here. For the sake of completeness, the result is given for γ arbitrary, although from a practical point of view most interest centres on the limiting cases of $\gamma = 0$ and $\gamma = \pi/2$.

An interesting outcome of this analysis is the discovery of two identities, which may be of use elsewhere.

A.1 Evaluation of the Integral

Expanding $\cos(ks\cdot\cos\beta\cdot\sin\gamma)$ and $J_o(ks\cdot\cos\gamma\cdot\sin\beta)$ as infinite power series in $\cos\beta$ and $\sin\beta$ respectively,

$$I_1 = \sum_{i=0}^{\infty}\sum_{j=0}^{\infty}\int_0^{\pi/2} \cos^{2m-1}\beta\cdot\sin\beta\cdot\exp(-Az\cdot\sec\beta)\ \frac{(-k^2s^2\sin^2\gamma\cdot\cos^2\beta)^i}{(2i)!}$$

$$\frac{(-k^2s^2\cos^2\gamma\cdot\sin^2\beta/4)^j}{j!\,j!}\ d\beta \ .$$

The term $(\sin^2\beta)^j$ has a binomial expansion in $\cos^2\beta$, i.e. $(1-\cos^2\beta)^j$. Doing this, and collecting like terms together

$$I_1 = \sum_{i=0}^{\infty}\sum_{j=0}^{\infty}\sum_{t=0}^{j}\int_0^{\pi/2} \frac{(-)^{i+2j-t}(k^2s^2)^{i+j}\sin^{2i}\gamma(\cos\gamma/2)^{2j}\cdot\cos\beta^{2m+2i+2j-2t-1}}{(2i)!\,j!\,t!\,(j-t)!}$$

$$\sin\beta\ \exp(-Az\cdot\sec\beta)\ d\beta \ . \qquad \text{(Eq. A.2)}$$

But in $\int_0^{\pi/2} \cos^N\beta\cdot\sin\beta\cdot\exp(-Az\cdot\sec\beta)\,d\beta$, putting sec = t this integral becomes

$$\int_1^\infty \frac{\exp(-Azt)}{t^{N+2}}\,dt$$

= the exponential integral $E_{N+2}(Az)$. (Eq. A.3)

Applying this to Eq. A.2, gives

$$I_1 = \sum_{i=0}^{\infty}\sum_{j=0}^{\infty}\sum_{t=0}^{j} \frac{(-)^{i-t}(k^2s^2)^{i+j}\sin^{2i}\gamma(\cos\gamma/2)^{2j}\,E_{2m+2i+2j-2t+1}(Az)}{(2i)!\,j!\,t!\,(j-t)!}.$$

Write t = j-n and sum over j and n. Since $t \geq 0$ and $j \geq n$,

$$I_1 = \sum_{i=0}^{\infty}\sum_{n=0}^{\infty}\sum_{j=n}^{\infty} \frac{(-)^{i+n-j}(k^2s^2)^{i+j}\sin^{2i}\gamma(\cos\gamma/2)^{2j}\,E_{2m+2i+2n+1}(Az)}{(2i)!\,j!\,(j-n)!\,n!}$$

(The change in order of summation is justified since it is easily seen that the triple summation is absolutely convergent.)

Now put j = n + r

$$I_1 = \sum_{i=0}^{\infty}\sum_{n=0}^{\infty}\sum_{r=0}^{\infty} \frac{(-)^{i-r}(k^2s^2)^{i+n+r}\sin^{2i}\gamma(\cos\gamma/2)^{2n+2r}\,E_{2m+2i+2n+1}(Az)}{(2i)!\,n!\,r!\,(n+r)!}$$

But

$$J_n(z) = (z/2)^n \sum_{r=0}^{\infty} \frac{(-z^2/4)^r}{r!\,(n+r)!},$$

and so the expression becomes, on summing over r,

$$I_1 = \sum_{i=0}^{\infty}\sum_{n=0}^{\infty} \frac{(-k^2s^2\gamma\cdot\sin^2\gamma)^i}{(2i)!}\,\frac{(ks\cdot\cos\gamma/2)^n}{n!}\,J_n(ks\cdot\cos\gamma)\,E_{2m+2i+2n+1}(Az)$$

(Eq. A.4)

Equation A.4 is the required closed form. As written, it is a Fourier-Bessel expansion

$$I_1 = \sum_{n=0}^{\infty} A_n\,J_n(ks\cdot\cos\gamma)$$

in which

$$A_n = \frac{(ks\cdot\cos\gamma/2)^n}{n!} \sum_{i=0}^{\infty} \frac{(-k^2s^2\cdot\sin^2\gamma)^i}{(2i)!} E_{2m+2i+2n+1}(Az) .$$

For computing, however, it may be better to expand in a series of exponential integrals. Writing i + n = p in Eq. A.4, I_1 becomes

$$\sum_{p=0}^{\infty} B_p E_{2m+2p+1}(Az),$$

where

$$B_p = \sum_{n=0}^{p} \frac{(-k^2s^2\cdot\sin^2\gamma)^{p-n}}{(2p-2n)!} \frac{(ks\cdot\cos\gamma/2)^n}{n!} J_n(ks\cdot\cos\gamma)$$

The coefficient B_p contains only a finite number of terms, which may be an advantage.

This general form will not be examined in further detail; as stated in the main text, the significant cases are those for which $\gamma = 0$ and $\gamma = \pi/2$. Each of these leads to a significant simplification in the expression for I_1.

A.2 Significant Cases

A.2.1 Horizontal Array ($\gamma = 0$)

In this case, from Eq. A.4, in the summation over i the only non-zero term is that for which i = 0, giving

$$I_1(\gamma = 0) = \sum_{n=0}^{\infty} \frac{(ks/2)^n}{n!} J_n(ks) E_{2m+2n+1}(Az). \qquad \text{(Eq. A.5)}$$

This is evidently a convergent series, since for n > 0 the moduli of both the Bessel function and the exponential integral are less than unity, so that the moduli of successive terms in n are less than $\frac{(ks/2)^n}{n!}$ i.e. less than the corresponding terms of the absolutely convergent series for exp(ks/2).

Numerical Computation

The following remarks will be superfluous to those who are practiced in numerical techniques, but may be useful to those who are not specialists, and who (as has happened so often to the author) can easily produce invalid answers.

In summing a convergent series of the form $u_o+u_1+y_2+\ldots+u_n\ldots$ it is customary to select a desired accuracy ε (e.g. $\varepsilon = 10^{-3}$ for accuracy to the third decimal place), and to terminate the series when $|u_n| < \varepsilon$. This assumes, however (among other things) that $|u_n|$ decreases monotonically with n. This condition is not necessarily true for the series of Eq. A.5.

First, $J_n(ks)$ is an oscillatory term; i.e., it passes through zero.

If, for example, ks happened to be equal to, or close to, a value corresponding to a zero of $J_n(ks)$, the naive application of the rule $|u_n| < \varepsilon$ would stop the series at n = 1, irrespective of the error.

Secondly, the criterion $|u_n| < \varepsilon$ is, in any case, only fully justified if the series consists of terms alternatively positive and negative. (For example, the series $\sum_{n=1}^{\infty} \frac{1}{n}$ diverges to infinity, and stopping at n = 100 does not give an answer correct to two decimal places.)

These difficulties may be overcome by finding an upper bound to the residue obtained by terminating the summation at the n'th term.

Since, for the purpose in the main text, the required quantity is normalized by dividing by the value of I_1 for ks = 0, viz $E_{2m+1}(Az)$, we have

$$\frac{I_1}{I_o} = \sum_{n=0}^{\infty} u_n$$

where

$$u_n = \frac{(ks/2)^n}{n!} J_n(ks) \cdot \frac{E_{2m+2n+1}(Az)}{E_{2m+1}(Az)} .$$

Hence the modulus of the residue R on stopping at the nth term is

$$R = \left| \sum_{r=n+1}^{\infty} u_n \right| \leq \sum_{r=n+1}^{\infty} |u_n| .$$

Now

$$J_n(ks) < 1 \quad \text{for } n > 0$$

and

$$\frac{E_{2m+2n+1}(Az)}{E_{2m+1}(Az)} < 1 \qquad \text{for } n > 0.$$

Hence

$$|u_r| < \frac{(ks/2)^n}{n!}$$

and

$$|R| < \frac{(ks/2)^{n+1}}{(n+1)!} + \frac{(ks/2)^{n+2}}{(n+2)!} + \ldots$$

$$= \frac{(ks/2)^{n+1}}{(n+1)!} \left[1 + \frac{(ks/2)}{n+2} + \frac{(ks/2)^2}{(n+3)(n+2)} + \ldots\right]$$

$$< \frac{(ks/2)^{n+1}}{(n+1)!} \left[1 + \frac{(ks/2)}{n+2} + \frac{(ks/2)^2}{(n+2)^2} + \ldots\right]$$

$$= \frac{(ks/2)^{n+1}}{(n+1)!} \; \frac{1}{1 - \frac{(ks/2)}{(n+2)}} .$$

A sufficient condition for terminating the summation is thus

$$\frac{(ks/2)^{n+1}}{(n+1)!} \times \frac{1}{1 - \frac{(ks/2)}{n+2}} < \varepsilon . \qquad \text{(Eq. A.6)}$$

This does not give unmanageable quantities. For example, if ks = 6, n = 12 gives an error $< 0.3 \times 10^{-3}$ and n = 13, an error $< 7 \times 10^{-5}$.

Two identities

If Az = 0 in Eq. A.5

$$I_1(\gamma = 0,\ Az = 0) = \sum_{n=0}^{\infty} \frac{(ks/2)^n}{n!} \; \frac{Jn(ks)}{2(m+n)}$$

(since $E_\mu(0) = \frac{1}{\mu-1}$).

Putting γ = Az = 0 in the original equation (Eq. A.1) gives

$$I_1(\gamma = 0,\ Az = 0) = 2 \int_0^{\pi/2} \cos^{2m-1}\beta \cdot \sin\beta \cdot J_0(ks \cdot \sin\beta)\, d\beta .$$

But this is a known integral (see <A2> for example), which integrates to

$$I_1(\gamma = 0,\ Az = 0) = 2^{m-1}(m-1)!\ J_m(ks)(ks)^{-m}$$

and so we have the identity

$$J_m(ks) \equiv \frac{(ks/2)^m}{(m-1)!} \sum_{n=0}^{\infty} \frac{(ks/2)^n J_n(ks)}{(m-n)\cdot n!} \qquad \text{(Eq. A.7)}$$

which, oddly enough, expresses $J_m(ks)$ as a Fourier-Bessel series.

From Eq. A.7 an algebraic identity can be deduced. Expanding the Bessel functions as power series in ks

$$(ks/2)^m \sum_{r=0}^{\infty} \frac{(-k^2s^2/4)^r}{r!\,(m+r)!} = \frac{(ks/2)^m}{(m-1)!} \sum_{n=0}^{\infty} \sum_{t=0}^{\infty} \frac{(ks/2)^{2n}}{(m+n)\cdot n!} \frac{(-k^2s^2/4)^t}{t!\,(n+t)!}$$

or

$$\sum_{r=0}^{\infty} \frac{(-)^r(k^2s^2/4)^r}{r!\,(m+r)!} = \frac{1}{(m-1)!} \sum_{n=0}^{\infty} \sum_{t=0}^{\infty} \frac{(-)^t(k^2s^2/4)^{n+t}}{(m+n)\cdot n!\,t!\,(n+t)!} \ ,$$

writing n + t = r, the second term becomes

$$\frac{1}{(m-1)!} \sum_{r=0}^{\infty} \sum_{n=0}^{r} \frac{(-)^{r-n}(k^2s^2/4)^r}{(m+n)\cdot!\,r!\,(r-n)!} \ .$$

Equating terms in $(k^2s^2/4)^r$.

$$\frac{1}{(m+r)!\,r!} = \frac{1}{(m-1)!} \sum_{n=0}^{r} \frac{(-)^n}{(m+n)n!\,r!\,(r-n)!}$$

or

$$\frac{1}{m(m+1)(m+2)\dots(m+r)} = \sum_{n=0}^{r} \frac{(-)^n}{(m+n)r!\,(r-n)!} \ , \qquad \text{(Eq. A.8)}$$

a relationship which is surprisingly difficult to establish by purely algebraic methods.

A.2.2 Vertical Array ($\gamma = \pi/2$)

A similar simplification is introduced by setting $\gamma = \pi/2$. In this case, in Eq. A.4, the only non-zero term in the summation over n is that for which n = 0, yielding

$$I_1(\gamma = \pi/2) = \sum_{i=0}^{\infty} \frac{(-k^2s^2)^i}{(2i)!} E_{2m+2i+1}(Az) \ . \qquad \text{(Eq. A.9)}$$

This is an even simpler form than for the horizontal array. The factors $\dfrac{(-k^2s^2)^i}{(2i)!}$ are the terms in the expansion of cos(ks).

The computation is similarly somewhat simpler. As for the horizontal array there is a terminal condition that

$$\frac{(ks)^{2i+2}}{(2i+2)!} < \frac{(ks)^i}{(2i)!}$$

or

$$(2i+2)(2i+1) > k^2s^2 ,$$

which is certainly the case if

$$(2i+1) > ks$$

or

$$i > (ks-1)/2.$$

Moreover, since terms alternate in sign, a sufficient condition for an error not exceeding ε is

$$\frac{(k^2s^2)^{i+1}}{(2i+2)!} \cdot \frac{E_{2m+2i+1}(Az)}{E_{2m+1}(Az)} < \varepsilon . \qquad \text{(Eq. A.10)}$$

REFERENCES

A.1 ABRAMOWITZ, M. and STEGUN, I.A. Handbook of Mathematical Functions. Washington DC, US Dept. of Commerce National Bureau of Standards, 1965.

A.2 CRON, B. and SHERMAN, C.H. Spatial correlation functions for various noise models. Journal Acoustical Society of America, 34, 1962: 1732-1736.

APPENDIX B

EVALUATION OF THE INTEGRAL GIVING THE AMBIENT NOISE POWER IN THE OUTPUT OF A CONVENTIONAL BEAMFORMER

In the main text Eq. 4c includes the following double integral:

$$I_2 = \int_0^{\pi/2} \int_0^{2\pi} \cos^{2m-1}\beta \cdot \sin\beta \cdot \exp(-Az \cdot \sec\beta)\, [f(P)F(Q)]^2 \, d\phi \, d\beta \,, \qquad \text{(Eq. B.1)}$$

where m is a non-negative integer,

Az is a positive constant,

$$f(P) = \frac{\sin(Px/2)}{P \sin(x/2)} \,, \qquad F(Q) = \frac{\sin(Qy/2)}{Q \sin(y/2)} \,,$$

with $x = ks \cdot \sin\beta \cdot \cos\phi$,

$y = ks(\sin\beta \cdot \cos\gamma \cdot \sin\phi - \sin\gamma \cdot \cos\beta + \sin\theta)$.

The first stage is the integration with regard to ϕ, which involves only the factor in squared brackets. To start with we find an expression for $f^2(P)$ in terms of the weighted sum of a number of terms of the form $\cos(rx)$. To show that this is possible, consider the trigonometric identify:

$$\sin(Px/2) - \sin(\overline{P-2} \cdot x/2) = 2\cos(\overline{P-1} \cdot x/2) \cdot \sin(x/2)$$

and therefore

$$\sin(\overline{P-2}) \cdot x/2) - \sin(\overline{P-4} \cdot x/2) = 2\cos(\overline{P-3} \cdot x/2) \cdot \sin(x/2), \text{ etc.}$$

terminating with

$$\sin(2x/2) - \sin(0) = 2\cos(x/2)\sin(x/2) \quad [P \text{ even}]$$

$$\sin(3x/2) - \sin(x/2) = 2\cos(2x/2)\sin(x/2) \quad [P \text{ odd}].$$

Summing,

$$\frac{\sin(Px/2)}{\sin x/2} = 2[\cos(\overline{P-1}) \cdot x/2) + \cos(\overline{P-3} \cdot x/2) + \ldots] \qquad \text{(Eq. B.2)}$$

the summation ending with $\cos(x/2)$ [P even]

1/2 [P odd].

On squaring, $\dfrac{\sin^2(Px/2)}{\sin^2(x/2)}$ will contain terms of the form

$$\cos(rx/2)\cos(tx/2) = \tfrac{1}{2}[\cos(\overline{r+t})\cdot x/2) + \cos(r-t)\cdot x/2].$$

But r and t are either both odd or both even, so that $\frac{1}{2}(r+t)$ and $\frac{1}{2}(r-t)$ are both integers. It follows that

$$\frac{\sin^2(Px/2)}{\sin^2(x/2)} = \sum_{r=0}^{P-1} A_r \cos(rx) \qquad \text{(Eq. B.3)}$$

[since, on squaring Eq. B.2, the highest order term will be cos(P-1)x].

To evaluate the coefficients A_r in Eq. B.3, note that

$$\frac{\sin^2(Px/2)}{\sin^2(x/2)} = \frac{1-\cos Px}{1-\cos x},$$

so that

$$1-\cos Px = (1-\cos x)\sum_{r=0}^{P-1} A_r\cdot\cos(rx)$$

$$= \sum_{r=0}^{P-1} A_r\cdot\cos(rx) - A_o\cdot\cos x - \tfrac{1}{2}\sum_{r=1}^{P-1} A_r[\cos(\overline{r+1}x) + \cos(\overline{r-1}x)].$$

Equating coefficients of cos(rx),

$$A_o - \tfrac{1}{2}A_1 = 1,$$

$$A_1 - \tfrac{1}{2}A_2 - A_o = 0,$$

$$A_r - \tfrac{1}{2}A_{r-1} - \tfrac{1}{2}A_{r+1} = 0 \qquad 2 \le r \le P-2,$$

$$A_{P-1} - \tfrac{1}{2}A_{P-2} = 0,$$

$$\tfrac{1}{2}A_{P-1} = 1.$$

It is easy to show that the solution of these equations is

$$A_o = P,$$

$$A_r = 2(P-r) \quad 1 \le r < P-1.$$

Similarly

$$\frac{\sin^2(Qy/2)}{\sin^2(y/2)} = \sum_{t=0}^{Q-1} B_t \cdot \cos(ty),$$

where

$$B_o = Q,$$

$$B_t = 2(Q-t) \quad 1 \leq t \leq Q-1 .$$

Therefore

$$P^2Q^2[f(P)\cdot f(Q)] \quad \sum_{r=0}^{P-1} \sum_{t=0}^{Q-1} A_r B_t \cos(rx)\cdot\cos(ty)$$

$$= \tfrac{1}{2} \sum_r \sum_t A_r B_t [\cos(rx+ty) + \cos(rx-ty)].$$

Now consider the integral of cos(rx+ty) with respect to ϕ.

$$rx+ty = ks[r\cdot\sin\beta\cdot\cos\phi + t(\sin\beta\cdot\cos\gamma\cdot\sin\phi - \sin\gamma\cdot\cos\beta + \sin\theta]$$

$$= ks[\sin\beta \sqrt{r^2+t^2\cos^2\gamma}\cdot\sin(\phi+\varepsilon) - t(\sin\gamma\cdot\cos\beta - \sin\theta)],$$

where

$$\tan\varepsilon = r/(t\cdot\cos\gamma).$$

Therefore

$$\cos(rx+ty) = \cos(ks\cdot\sin\beta \sqrt{r^2+t^2\cos^2\gamma}\cdot\sin\overline{\phi+\varepsilon})\cdot\cos[kst(\sin\gamma\cdot\cos\beta - \sin\theta]$$

$$+ \sin(ks\cdot\sin\beta \sqrt{r^2+t^2\cos^2\gamma}\cdot\sin\overline{\phi+\varepsilon})\cdot\sin[kst(\sin\gamma\cdot\cos\beta - \sin\theta].$$

But, in integrating over 2π, since the integrand is periodic with period 2π, the phase term ε does not appear in the result, and may be therefore set equal to zero.

Further, in forming cos(rx-ty), it is necessary only to change the sign of t, which will leave the cosine term unaltered, but will change the sign of the sine term. The latter therefore vanishes identically on adding, and

$$P^2Q^2 \int_o^{2\pi} [f(P)\cdot f(Q)]^2 d\phi = \sum_r \sum_t \int_o^{2\pi} A_r B_t \cdot\cos[kst(\sin\gamma\cdot\cos\beta - \sin\theta] \cos(\lambda\cdot\sin\beta\cdot\sin\phi)\, d\phi$$

where $\lambda = ks\sqrt{r^2+t^2\cos^2\gamma}$

$$= 2\pi \sum_r \sum_t A_r B_t \cdot \cos[kst(\sin\gamma\cdot\cos\beta - \sin\theta] J_o(\lambda\cdot\sin\beta)$$

$$= 2\pi \sum_r \sum_t A_r B_t J_o(\lambda\cdot\sin\beta)[\cos(kst\cdot\sin\theta)\cos(kst\cdot\sin\gamma\cdot\cos\beta) + \sin(kst\cdot\sin\theta)\sin(kst\cdot\sin\gamma\cdot\cos\beta)],$$

and therefore

$$\frac{P^2Q^2}{2\pi} I_2 = \sum_{r=0}^{P-1} \sum_{t=0}^{Q-1} \int_o^{\pi/2} A_r B_t [\cos p\cdot\cos(q\cos\beta)+\sin p\cdot\sin(q\cdot\cos\beta)] J_o(\lambda\cdot\sin\beta) \times \cos^{2m-1}\beta\cdot\sin\beta\cdot\exp(-Az\cdot\sec\beta)\, d\beta \ ,$$

where

$$p = kst\cdot\sin\theta$$

$$q = kst\cdot\sin\gamma$$

$$\lambda = ks\sqrt{r^2+t^2\cos^2\gamma} \ .$$

Now the integral involving $\cos(q\cdot\cos\beta)$ is of the same form as that for evaluating the integral I_1 discussed in Appendix A, and we may write immediately the first term as (see Eq. A.4 of App. A).

$$\sum_{i=0}^{\infty} \sum_{n=0}^{\infty} \sum_{r=0}^{P-1} \sum_{t=0}^{Q-1} A_r B_t \cdot \cos p \frac{(-q^2)^i}{(2i)!} \cdot \frac{(\lambda/2)^n}{n!} \cdot J_n(\lambda)\, E_{2m+2i+2n+1}(Az).$$

Moreover, in forming the second integral, it is sufficient to note that since

$$\cos(q\cdot\cos\beta) = \sum_{i=0}^{\infty} \frac{(-q^2\cos^2\beta)^i}{(2i)!}$$

and

$$\sin(q\cdot\cos\beta) = \sum_{i=0}^{\infty} (-i)^i \frac{(q\cdot\cos\beta)^{2i+1}}{(2i+1)!}$$

$$= q\cdot\cos\beta \sum_{i=0}^{\infty} \frac{(-q^2\cos^2\beta)^i}{(2i+1)!} \ ,$$

this term derives immediately from the first by writing 2m+1 for 2m and writing (2i+1) for (2i).

Thus finally,

$$\frac{P^2Q^2}{2\pi} I_2 = \sum_{i=0}^{\infty} \sum_{n=0}^{\infty} \sum_{r=0}^{P-1} \sum_{t=0}^{Q-1} A_r B_t (-)^i \cdot \frac{(\lambda/2)n}{n!} J_n(\lambda) \cdot \frac{\cos p \cdot q^{2i}}{(2i)!} E_{2m+2n+2i+1}(Az)$$

$$+ \frac{\sin p \cdot q^{2i+1}}{(2i+1)!} E_{2m+2n+2i+2}(Az) \quad ,$$

(Eq. B.4)

where

$A_o = P$ $\qquad B_o = Q$

$A_r = 2(P-r) \quad [r>0]$ $\qquad B_t = 2(Q-t) \quad [t>0]$

$\lambda = ks \sqrt{r^2+t^2\cos^2\gamma}$

$p = kst \cdot \sin\theta$

$q = kst \cdot \sin\gamma$

This formidable quadruple integral is the formal solution of the double integral. The general form (Eq. B.4) has been derived for the sake of completeness although it does not appear to be inviting for numerical computation. It is not, however, impossible. Comparing with the equivalent form for I_1 (Eq. A.4 of App. A), it is evident that, for given n and i, Eq. A.4 requires only one Bessel function and one exponential integral to be computed. In the present integral it is immediately evident that PQ Bessel functions will need to be evaluated, two exponential integrals, and 2PQ coefficients of the form $A_r B_t q^{2i}$ or $A_r B_t q^{2i+1}$. For PQ large this would be a formidable undertaking.

However, it is probably much more important to look at the special cases of $\gamma = 0$ and $\gamma = \pi/2$.

Making $\gamma = 0$ does yield notable simplification. Since $q = 0$, the only surviving term in the summation over i is the first term in Eq. B.4 for $i = 0$, so that

$$I_2 \; (\gamma=0) = \frac{2\pi}{P^2Q^2} \sum_{n=0}^{\infty} \sum_{r=0}^{P-1} \sum_{t=0}^{Q-1} A_r B_t \cdot \cos p \cdot \frac{(\lambda_1/2)^n}{n!} \cdot J_n(\lambda_1) E_{2m+2n+1}(Az),$$

(Eq. B.5)

where

$\lambda_1 = ks \sqrt{r^2+t^2}$ $\qquad p = kst \cdot \sin\theta$.

Comparing with the equivalent form for I_1 (Eq. A.5 of App. A), Eq. B.5 consists of a weighted sum of PQ simpler forms, so that a computer programme designed for I_1 could be used as a subroutine for I_2. This would be slightly wasteful in the computation of the Bessel Functions since, because of the symmetry of λ_1 in r and t, many may turn up twice. It is easy to show in fact, if R is the lesser of P and Q, the number of different Bessel functions to be calculated is $PQ-\frac{1}{2}(R-1)$. For P = Q, for example, this becomes $\frac{1}{2}P(P+1)$, a saving of nearly 50% for P large. However, the complication in programming for these replicas may offset such a saving.

Making $\gamma = \pi/2$ does not simplify quite so neatly. We now retain the quadruple summation, so that $I_2(\gamma = \pi/2)$ has the form of Eq. B.4, in which

$$\gamma_2 = ksr \qquad q = kst.$$

However, λ_2 does not involve t, so there are now only P terms of the form $\frac{(\lambda_2/2)^n}{n!} J_n(\lambda_2)$ to be computed.

INITIAL DISTRIBUTION

MINISTRIES OF DEFENCE	Copies
MOD Belgium	2
DND Canada	10
CHOD Denmark	8
MOD France	8
MOD Germany	15
MOD Greece	11
MOD Italy	10
MOD Netherlands	12
CHOD Norway	10
MOD Portugal	5
MOD Turkey	5
MOD U.K.	[illegible]6
SECDEF U.S.	[illegible]
NATO AUTHORITIES	
Defence Planning Committee	[illegible]
NAMILCOM	2
SACLANT	10
SACLANTREPEUR	1
CINCWESTLANT/COMOCEANLANT	[illegible]
COMIBERLANT	[illegible]
CINCEASTLANT	1
COMSUBACLANT	1
COMMAIREASTLANT	1
SACEUR	2
CINCNORTH	1
CINCSOUTH	1
COMNAVSOUTH	1
COMSTRIKFORSOUTH	1
COMEDCENT	1
COMMARAIRMED	1
CINCHAN	1

SCNR FOR SACLANTCEN	Copies
SCNR Belgium	1
SCNR Canada	1
SCNR Denmark	1
SCNR Germany	1
SCNR Greece	1
SCNR Italy	1
SCNR Netherlands	1
S[illegible] Norway	1
[illegible]al	1
[illegible]key	1
[illegible]	1
[illegible].S.	2
S[illegible] Rep. SCNR	1
NAMILCOM Rep. SCNR	1
NATIONAL LIAISON OFFICERS	
NLO Canada	1
[illegible]O Denmark	1
[illegible]ermany	1
[illegible]aly	1
[illegible]K.	1
[illegible].S.	1
NLR TO SACLANT	
NLR Belgium	1
NLR Canada	1
NLR Denmark	1
NLR Germany	1
NLR Greece	1
NLR Italy	1
NLR Netherlands	1
NLR Norway	1
NLR Portugal	1
NLR Turkey	1
NLR UK	1
NLR US	1

Total initial distribution	240
SACLANTCEN Library	10
Stock	30
Total number of copies	280